Magnetic Resonance in Medicine 44:731–736 (2000)

Rapid Isotropic Diffusion Mapping Without Susceptibility Artifacts: Whole Brain Studies Using Diffusion-Weighted Single-Shot STEAM MR Imaging

Ulrike G. Nolte, Jürgen Finsterbusch, and Jens Frahm*

A subsecond magnetic resonance imaging (MRI) technique for isotropic diffusion mapping is described which, in contrast to echo-planar imaging (EPI), is insensitive to resonance offsets, i.e., tissue susceptibility differences, magnetic field inhomogeneities, and chemical shifts. It combines a diffusion-weighted (DW) spin-echo preparation period and a high-speed stimulated echo acquisition mode (STEAM) MRI sequence and yields single-shot images within measuring times of 559 msec (80 echoes). Here, diffusion encoding involved one scan without DW, three DW scans with $b = 490$ sec mm^{-2}, and three DW scans with $b = 1000$ sec mm^{-2} (orthogonal gradient orientations). An automated on-line evaluation resulted in isotropic DW images as well as ADC maps (trace of the diffusion tensor). Experiments at 2.0 T covered the brain of healthy subjects in 20 contiguous sections of 6 mm thickness and 2.0 × 2.0 mm^2 in-plane resolution within a total measuring time of 78 sec. High-resolution studies at 1.0 × 1.0 mm^2 (interpolated from 2.0 × 1.0 mm^2 acquisitions) were obtained within 5 min 13 sec using four averages. In comparison with EPI, DW single-shot STEAM MRI exhibits only about half the SNR, but completely avoids regional signal losses, high intensity artifacts, and geometric distortions. Magn Reson Med 44:731–736, 2000. © 2000 Wiley-Liss, Inc.

Key words: magnetic resonance imaging; high-speed imaging; diffusion-weighted imaging; apparent diffusion coefficient; susceptibility artifacts

Diffusion contrast in MRI is gaining increasing importance in a variety of clinical applications ranging from cerebral ischemia to childhood disorders associated with disturbed myelination. Pertinent studies face two major challenges even in cases, such as acute stroke, in which a relatively simple parameter such as the bulk water diffusivity seems to be important in the assessment of neuroaxonal tissue integrity.

First, to circumvent ambiguities in the interpretation of diffusion-weighted (DW) images of structurally heterogenous tissues, it is mandatory to ensure an isotropic encoding of diffusion contrast independent of the relative directions of the applied gradients and the tissue components under investigation. Corresponding attempts need to determine the apparent diffusion coefficient (ADC), here defined as the trace of the diffusion tensor. Although it is possible to obtain an isotropic DW image in a single step, most studies employ multiple DW acquisitions with orthogonal gradient orientations because of an improved signal-to-noise ratio (SNR) and reduced T_2 weighting. Second, an effective reduction of the unavoidable sensitivity of DW MRI sequences to motion requires single-shot imaging. So far, most clinical applications have relied on echo-planar imaging (EPI) despite the fact that even "spin-echo" EPI is a gradient-echo technique that suffers from resonance offset effects. Pertinent signal alterations and geometric distortions, e.g., in the vicinity of air-tissue interfaces, become a serious and obvious problem when using DW EPI in whole brain studies covering the cortex, midbrain, cerebellum, and brainstem. Similar arguments apply for DW EPI of abdominal organs.

Thus, the purpose of this work was to develop an alternative single-shot MRI sequence which allows for rapid mapping of diffusion tensor properties without sensitivities to tissue susceptibility differences, magnetic field inhomogeneities, and chemical shifts. Potential candidates are gradient-echo MRI sequences with very short echo times or RF-refocused echo sequences based on spin echos (SEs) or stimulated echoes (STEs). Whereas combinations of diffusion encoding with turbo fast low angle shot (turboFLASH) require a multi-shot strategy to correct for phase shifts (1) and contamination with non-DW magnetizations caused by T_1 relaxation (2), single-shot rapid acquisition with relaxation enhancement (RARE) sequences (3) are hampered by the occurrence of two phase-shifted echo "families." In our experience, even the proposed split-echo half Fourier acquisition method (4) leads to residual motion problems in applications to the human brain. (For a more detailed analysis and experimental observations see Ref. 5).

Extending the search for an optimized MRI sequence which offers clinically robust diffusion mapping of the entire human brain, this work demonstrates a promising adaptation of a high-speed stimulated echo acquisition mode (STEAM) MRI sequence (6). The present solution (5) overcomes several limitations of a previously investigated sequence version (7), which originated mainly from the fact that the individual Fourier lines, i.e., STE signals, had different diffusion times varying over a range commensurable with the total acquisition time.

MATERIALS AND METHODS

DW Single-Shot STEAM MRI

Figure 1 shows the basic RF and magnetic field gradient pulse sequence for DW single-shot STEAM MRI. The technique employs a section-selective SE preparation period that replaces the leading 90° RF pulse of a conventional high-speed STEAM sequence (6). This 90°–180° RF excitation and refocusing period symmetrically encompasses three orthogonal diffusion gradients and results in an SE

Biomedizinische NMR Forschungs GmbH am Max-Planck-Institut für biophysikalische Chemie, Göttingen, Germany.

*Correspondence to: Jens Frahm, Ph.D., Biomedizinische NMR Forschungs GmbH, D-37070 Göttingen, Germany. E-mail: jfrahm@gwdg.de

Received 23 February 2000; revised 12 June 2000; accepted 19 June 2000.

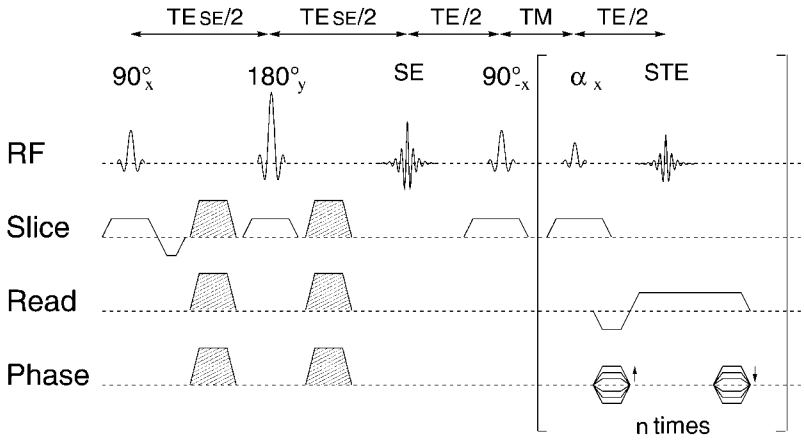

FIG. 1. The DW single-shot STEAM MRI sequence combines a section-selective SE preparation period (TE_{SE}) for diffusion encoding with a high-speed stimulated echo imaging module (TE of the STE signals). The bracket refers to the repetitive readout of n differently phase-encoded Fourier lines with use of low flip angle RF pulses (α).

signal the second half of which corresponds to the initial free induction decay signal of a normal STE sequence. Accordingly, the second 90° RF pulse recreates longitudinal magnetizations which are subsequently consumed as differently phase-encoded STE signals by a series of low flip angle RF pulses.

Similar to single-shot acquisitions in the presence of T_1 (turboFLASH) or T_2 (RARE) signal attenuation, centric reordering of the phase-encoding gradient table is favorable for the acquisition of STE signals that decay with T_1. However, the choice of a proper flip angle is a more important parameter because it dominates the intensity variation along the train of STE signals. Whereas very low flip angles (e.g., ≤ 8°) waste residual longitudinal magnetization, high flip angles (e.g., ≥ 14°) shift most of the available signal to the initially recorded low spatial frequencies at the expense of higher frequencies that define image sharpness. The flip angle for the read-out intervals was therefore theoretically optimized and adjusted to 11° for an acquisition matrix with 80 excitations of STE signals. The selection criteria were maximum SNR and minimum image blurring which would arise from a modulation of the point spread function. Possible improvements with use of variable flip angles were not implemented because of technical constraints.

Figure 2 summarizes the flip angle considerations. The top traces show the transverse magnetization M_{xy} as a function of echo number n ($1 \le n \le n_{max} = 80$) for three flip angles (α = 8, 11, and 14°) according to

$$M_{xy}(n) \propto (e^{-TR/T1} \cdot \cos\alpha)^{n-1} \cdot \sin\alpha. \quad [1]$$

Here, TR refers to the duration of the echo interval in the high-speed STEAM MRI sequence which typically is less than 10 msec. To express the transverse magnetization as a function of k along the phase-encoding dimension of k-space, centric reordering requires an assignment of odd and even echoes to either the negative or positive part of k-space. Hence

$$k(n) = -\frac{n-1}{2}\Delta k \quad \text{for } n \text{ odd } (k \le 0) \quad [2a]$$

$$k(n) = \frac{n}{2}\Delta k \quad \text{for } n \text{ even } (k > 0) \quad [2b]$$

with the field-of-view (FOV) determining the k-space increment Δk according to $\Delta k \cdot FOV = 2\pi$. Thus, the magnetization reads

$$M_{xy}(k) \propto (e^{-TR/T1} \cdot \cos\alpha)^{-2k/\Delta k} \cdot \sin\alpha \quad \text{for } (k \le 0) \quad [3a]$$

$$M_{xy}(k) \propto (e^{-TR/T1} \cdot \cos\alpha)^{2k/\Delta k - 1} \cdot \sin\alpha \quad \text{for } (k > 0). \quad [3b]$$

The signal decay in k-space is approximately symmetric as $(e^{-TR/T1} \cdot \cos\alpha)^{-1} \approx 1$. It may therefore be given in the exponential form

$$M_{xy}(k) \propto e^{-(TR/T1 - \ln\cos\alpha)2|k|/\Delta k} \cdot \sin\alpha \quad [4]$$

which is plotted in the middle traces of Fig. 2. Fourier transformation of Eq. [4] yields the desired point spread function shown in the lower traces of Fig. 2. The full width at half maximum (FWHM) is given by

$$FWHM = \frac{2 \cdot FOV}{\pi}(TR/T1 - \ln\cos\alpha). \quad [5]$$

The dominant factor in Eq. [5] is the second term in the bracket, i.e., the flip angle dependence, whereas differences in T_1 relaxation cause only negligible variations in resolution, e.g., between gray and white matter. For the experimental conditions used here, a flip angle of 11° provides a tolerable degree of blurring (about 2.5 mm resolution along the phase-encoding dimension of the image, in conjunction with an intermediate SNR (compare Fig. 2 top and middle traces)). A flip angle of 8° would not cause any damage to the nominal resolution by broadening the point spread function, but would significantly sacrifice SNR. On the other hand, the blurring to 3.7 mm obtained for a flip angle of 14° was not considered acceptable despite a formal gain in SNR.

Isotropic Diffusion Mapping

The calculation of an isotropic DW image and an ADC map employed an optimized gradient scheme consisting of 3 orthogonal gradient pairs with amplitude ratios of the x-, y-, and z-gradients of 2 : 2 : (−1), 2 : (−1) : 2, and (−1) : 2 : 2, respectively (8). The ADC map was chosen to represent the trace of the diffusion tensor, which is defined as the

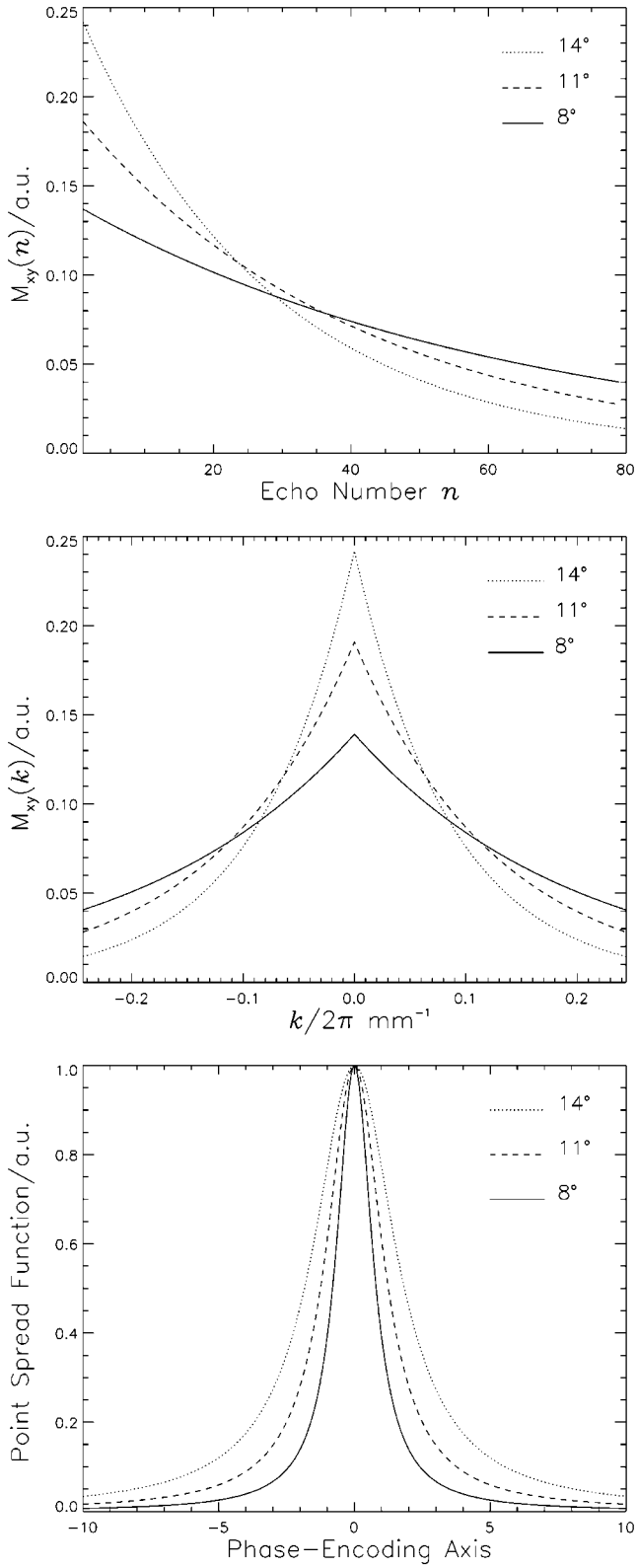

FIG. 2. Transverse magnetization M_{xy} as a function of top: echo number n (n_{max} = 80) and middle: k along the phase-encoding axis (according to Eqs. [1] and [4], respectively, for TR/T1 = 0.006, FOV = 160 mm in phase direction, and flip angles α = 8, 11, and 14°). Bottom: Normalized point spread functions obtained by Fourier transformation of Eq. [4].

weighted average of the diagonal elements D_{xx}, D_{yy}, and D_{zz} of the diffusion tensor according to

$$ADC = \frac{1}{3}(D_{xx} + D_{yy} + D_{zz}). \quad [6]$$

Because the diffusion protocol comprised a total of seven acquisitions per section (one scan without DW as well as three DW scans with b = 490 sec mm^{-2} and three DW scans with b = 1000 sec mm^{-2}), the diagonal elements were calculated from a least-squares fitting procedure according to Ref. 9. The diffusion weighting factor b is given by

$$b = \gamma^2 g^2 \delta^2 \left(\Delta - \frac{\delta}{3}\right) \quad [7]$$

with γ the gyromagnetic ratio, g the strength and δ the duration of the diffusion gradient, and Δ the diffusion time. For a maximum gradient strength per axis of g = 18.8 mT m^{-1}, the experimental values were δ = 26 msec, Δ = 35 msec, and TE_{SE} = 66 msec. The first middle interval was TM = 9.26 msec, and the echo interval was TR = 6.0 msec.

As a benefit of the effective decoupling of diffusion and imaging gradients by separate DW SE and STEAM MRI modules (Fig. 1), the method minimizes the influence of respective cross terms. The only residual overlap originates from the slice-selection gradient underlying the 180° RF pulse of the SE part and amounts to less than 1 sec mm^{-2}. This feature represents a major technical advancement over a previous sequence version (7) which increased both the diffusion time Δ and b factor with increasing echo number, and therefore also led to enhanced motion sensitivity.

Although the use of multiple b factors and/or gradient orientations easily extends the approach to full diffusion tensor mapping, this first study focused on a relatively fast protocol which in a clinical setting would be adequate for the detection of acute cerebral ischemia. An on-line algorithm for a pixel-by-pixel calculation of diffusion tensor properties was added to the image reconstruction software of the scanner. For the present work the automated evaluation included an isotropic DW image at the desired b factor, i.e., 1000 sec mm^{-2}, as an orientation-independent measure of microscopic water mobility, and an ADC map representing the trace of the diffusion tensor.

Human Studies

All studies were performed at 2.0 T using a conventional MRI system (Siemens Vision, Erlangen, Germany) equipped with 25 mT m^{-1} gradients and a maximum slew rate of 40 T m^{-1} sec^{-1}. Images of healthy young adults were acquired with use of the standard head coil. Written, informed consent was obtained in all cases before the examinations. Neither cardiac gating nor special head restraints were applied.

DW single-shot STEAM images were obtained in 559 msec for a 80 × 128 or 80 × 256 pixel matrix covering a rectangular 160 × 256 mm^2 FOV. Thus, the in-plane resolution was either 2.0 × 2.0 mm^2 or 1.0 × 1.0 mm^2 (interpolated from 2.0 × 1.0 mm^2 acquisitions). Whole brain studies involved sequential multi-slice acquisitions

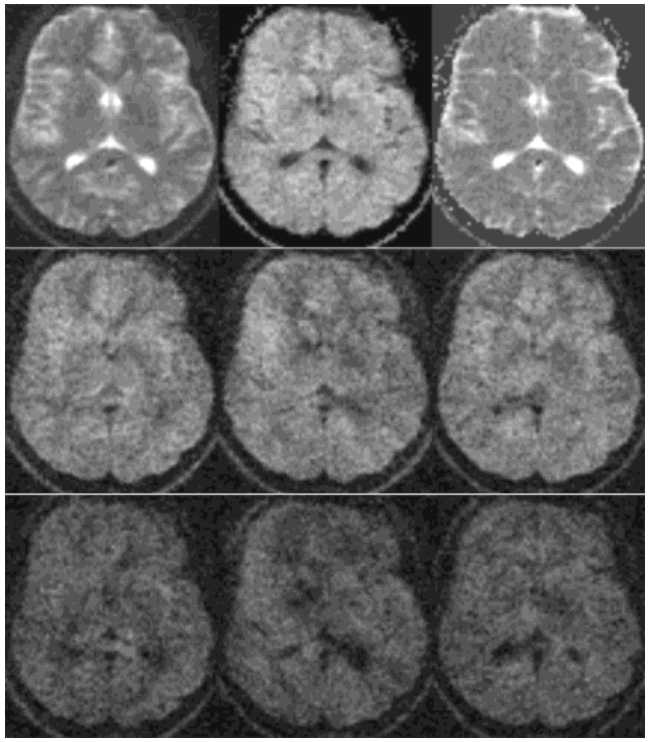

FIG. 3. DW single-shot STEAM MRI of the human brain. Top: Single-shot image without DW (left), calculated isotropic DW image at $b = 1000$ sec mm^{-2} (middle), and calculated ADC map (right). Middle: Single-shot DW scans in three orthogonal orientations at $b = 490$ sec mm^{-2}, and bottom: at $b = 1000$ sec mm^{-2}. The images represent a 6-mm-thick section at 2.0 × 2.0 mm^2 resolution (80 × 128 matrix, 160 × 256 mm^2 FOV, flip angle 11°, imaging time 559 msec).

of 20 contiguous sections of 6 mm thickness with interleaved excitation order (repetitions at ≈ 11 sec), and led to a total imaging time of about 78 sec.

DW STEAM MRI was compared to EPI using a DW sequence supplied by the manufacturer. The approach employed two b factors of 500 and 1000 sec mm^{-2} (mean echo time $TE_{SE} = 100$ msec) and resulted in DW images at 2.0 × 2.7 mm^2 resolution. For EPI, isotropic DW images were calculated by an off-line procedure.

RESULTS AND DISCUSSION

Figure 3 illustrates the strategy for determining isotropic DW images with use of single-shot STEAM MRI. For a single section, the seven raw acquisitions of the used diffusion protocol are shown in the top left image (one scan without DW), in the middle row (three DW scans along orthogonal gradient orientations at $b = 490$ sec mm^{-2}), and in the bottom row (three DW scans at $b = 1000$ sec mm^{-2}). It should be noted that the orientations of the diffusion gradients are not collinear with the imaging gradients, as the gradient scheme for DW takes advantage of an overlap of all three gradient axes to enhance the effective b factor for a given gradient duration and diffusion time. Intensity variations between the three DW scans in the middle and bottom row, respectively, are caused by anisotropic diffusion in white matter regions of the selected brain section.

The middle image in the top row of Fig. 3 is an isotropic DW image calculated at $b = 1000$ sec mm^{-2}. Its diffusion sensitivity is independent of the relative orientations of tissue components and diffusion gradients. With signal contributions from cerebral spinal fluid (CSF) effectively nulled by DW, and in the absence of tissue pathologies, the observed contrast mainly reflects T_2 differences between gray and white matter imposed during SE preparation. This isotropic DW image is the target scan for clinical applications as it provides the "background" for highlighting cerebral ischemic lesions with reduced water diffusivity, i.e., smaller ADC values. The top right image of Fig. 3 shows the corresponding calculated ADC map, which may be used for a quantitative assessment of ADC changes. It contains rather uniform ADC values for gray and white matter as well as high ADC values for CSF. Acute ischemic lesions would appear as dark areas of reduced ADC values.

Figures 4 and 5 depict isotropic DW STEAM MR images of whole brain studies of the same subject. The data illustrate the achievable image quality, SNR, spatial resolution, volume coverage, and total measuring time as key parameters for clinical applications. Whereas Fig. 4 emphasizes a short measuring time at a voxel resolution of 2.0 × 2.0 × 6.0 mm^3 or

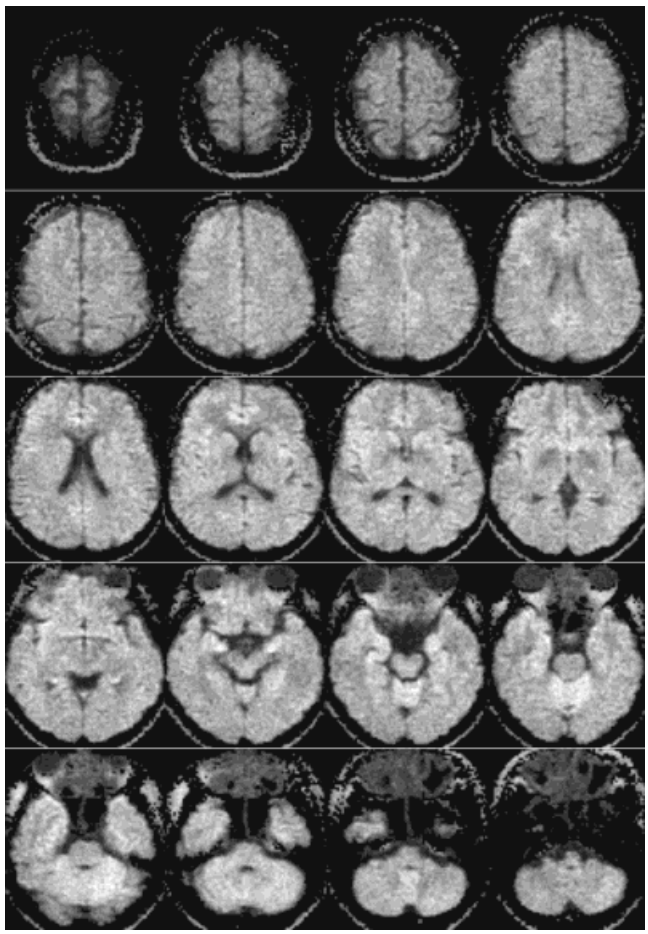

FIG. 4. Isotropic DW STEAM MR images ($b = 1000$ sec mm^{-2}) of the human brain at 2.0 × 2.0 mm^2 resolution. The total measuring time was 78 sec for 20 contiguous sections (other parameters as in Fig. 3).

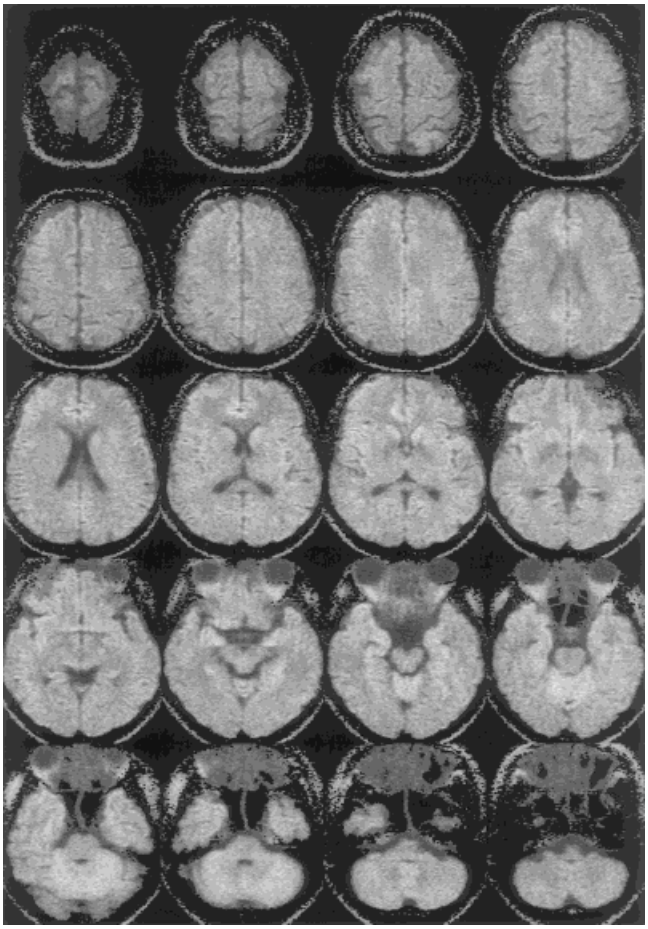

FIG. 5. Isotropic DW STEAM MR images (b = 1000 sec mm^{-2}) of the human brain at 1.0 × 1.0 mm^2 resolution (interpolated from 2.0 × 1.0 mm^2 acquisitions). The total measuring time was 5 min 13 sec for 20 contiguous sections (four averages, 80 × 256 matrix, other parameters as in Fig. 3).

24 μl, Fig. 5 employs a fourfold higher resolution of 1.0 × 1.0 × 6.0 mm^3 or 6 μl at the expense of a prolonged measuring time (four averages). Figure 5 clearly demonstrates the ability to reach a much higher spatial resolution than that typically obtained for single-shot DW EPI.

A most important feature of STEAM MR images is the complete absence of susceptibility artifacts, as was previously observed for a DW line scan variant (10). This aspect is evident in a direct comparison of isotropic DW STEAM and EPI images as shown for selected brain sections in the middle and right columns of Fig. 6, respectively. With reference to the anatomic fast SE images in the left column, and in contrast to the DW STEAM images, EPI reveals marked geometric distortions as well as pronounced intensity alterations. Pertinent artifacts appear mostly in applications of DW EPI to lower parts of the brain, but are also evident in sections through the midbrain and thalamus. In particular, the presence of susceptibility-induced high-intensity areas may cause a significant diagnostic problem, as these signals may be mistaken for ischemic lesions.

For the experimental conditions chosen in Fig. 6, and taking the differences in spatial resolution into account, a region-of-interest analysis revealed the SNR of single-shot STEAM MRI to be a factor of 1.7 lower than for EPI. Of course, signal averaging may be an option as whole brain studies are completed within 78 sec. On the other hand, it should be noted that only the absence of susceptibility artifacts guarantees a reliable calculation of orientation-independent parametric images such as isotropic diffusion maps, whereas EPI scans may be differently distorted for different diffusion gradient orientations and may therefore hamper or even preclude a common analysis.

CONCLUSION

DW single-shot STEAM MRI allows diffusion mapping without the geometric distortions or focal signal alterations shown by EPI in the presence of magnetic susceptibility differences. Easy access to isotropic DW via the trace of the diffusion tensor avoids complications caused by anisotropy in white matter regions. Together with the ability to image at

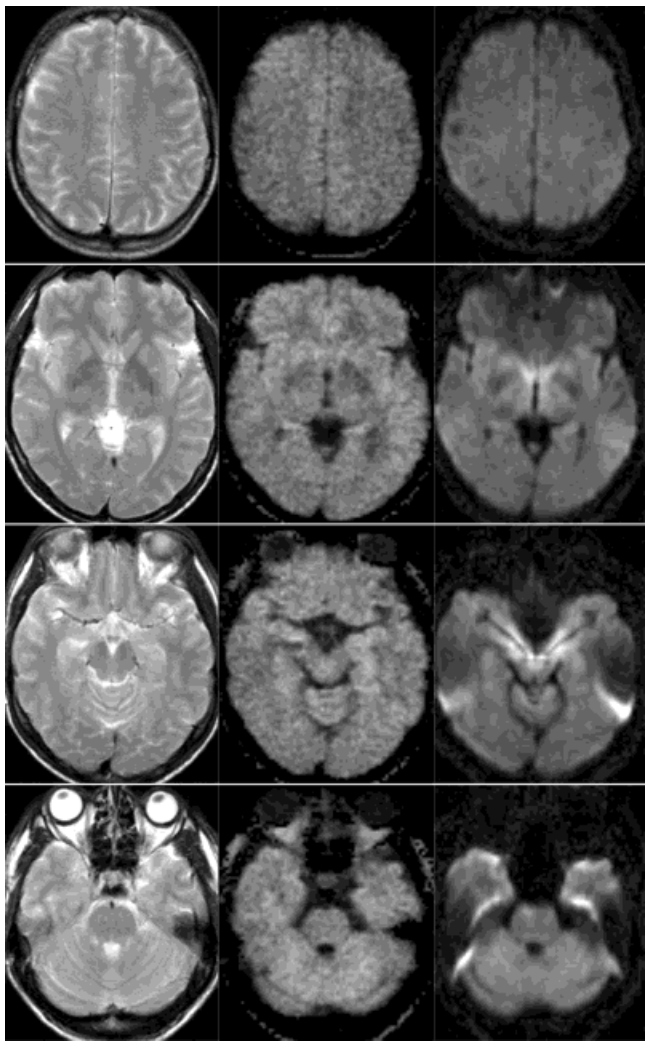

FIG. 6. DW MRI of the human brain in four sections (6 mm thickness) with different degrees of susceptibility affection. Left: Anatomic fast SE images (TR/TE = 2500/98 msec); middle: isotropic DW STEAM images (2.0 × 2.0 mm^2, b = 1000 sec mm^{-2}, other parameters as in Fig. 3); and right: isotropic DW EPI images (2.0 × 2.7 mm^2, b = 1000 sec mm^{-2}).

high spatial resolution, DW STEAM MRI promises to improve the diagnostic conspicuity of (small) ischemic lesions in arbitrary locations of the cortex, midbrain, cerebellum, or brainstem. The determination of a suitable compromise between SNR, spatial resolution, and measuring time for studies of patients with acute stroke is in progress.

The performance of the STEAM technique will clearly benefit from the use of higher magnetic fields: T_1 relaxation times tend to increase with field strength, while low flip angle excitations of stimulated echoes do not suffer from the increased RF power deposition or susceptibility problems found in high-field RARE or EPI, respectively. Extensions of DW single-shot STEAM MRI to full diffusion tensor mapping are straightforward, at the expense of measuring time.

REFERENCES

1. Thomas DL, Pell GS, Lythgoe MF, Gadian DG, Ordidge RJ. A quantitative method for fast diffusion imaging using magnetization-prepared turboFLASH. Magn Reson Med 1998;39:950–960.
2. Coremans J, Spanoghe M, Budinsky L, Sterckx J, Luypaert R, Eisendraht H, Osteaux M. A comparison between different imaging strategies for diffusion measurements with the centric phase-encoded turboFLASH sequence. J Magn Reson 1997;124:323–342.
3. Norris DG, Börnert P, Reese T, Leibfritz D. On the application of ultra-fast RARE experiments. Magn Reson Med 1992;27:142–164.
4. Schick F. SPLICE: sub-second diffusion-sensitive MR imaging using a modified fast spin-echo acquisition mode. Magn Reson Med 1997;38: 638–644.
5. Nolte U. Diffusionskodierende NMR-Tomografie des Gehirns. Diploma thesis, Georg-August Universität Göttingen, 1999.
6. Frahm J, Haase A, Matthaei D, Merboldt KD, Hänicke W. Rapid NMR imaging using stimulated echoes. J Magn Reson 1985;65:130–135.
7. Merboldt KD, Hänicke W, Gyngell ML, Bruhn H, Frahm J. Diffusion imaging of the human brain in vivo using high-speed STEAM MRI. Magn Reson Med 1992;23:179–192.
8. Gudbjartsson H, Maier SE, Mulkern RV, Mórocz IÁ, Patz S, Jolesz FA. Line scan diffusion imaging. Magn Reson Med 1996;36:509–519.
9. Pierpaoli C, Jezzard P, Basser PJ, Barnett A, Di Chiro G. Diffusion tensor MR imaging of the human brain. Radiology 1996;201:637–648.
10. Finsterbusch J, Frahm J. Diffusion-weighted single-shot line scan imaging of the human brain. Magn Reson Med 1999;42:772–778.